Error Compensation of Coordinate Measuring Machines

G. Zhang, Tianjin University/PRC, R. Veale, T. Charlton, B. Borchardt and R. Hocken (2), National Bureau of Standards, Gaithersburg, MD 20899

The methods and results are presented for applying software error compensation to a commercial three axis coordinate measuring machine. The technique incorporates compensation for geometric positioning errors and some thermal effects. Geometric error computation is based on a rigid body model of workpiece motion in the machine coordinate frame. Complete kinematic equations of the error motions are presented. The measurement method only requires taking a small set of data for each axis to compute the errors throughout the full workzone. To achieve the desired accuracy, squareness is determined using linear displacement measurements along selected machine diagonals. The dominant thermal effects in the machine are removed by introducing the concept of an "effective" nominal differential expansion coefficient. The entire error compensation computation is incorporated into the machine position reading subroutine to automatically produce compensated readings. The effectiveness of this method is tested by measuring linear displacement along arbitrarily oriented lines through the workzone and by measuring the length of a 500 mm gage block in several orientations. The results show a factor of ten performance improvement (limited by measurement repeatability) over 0.5 C range in temperature.

INTRODUCTION

We at the National Bureau of Standards have, for some years, been involved with error compensation of coordinate measuring machines and machine tools (Ref. 1). Recently we completed the error compensation of a typical industrial three-coordinate measuring machine, obtaining approximately a factor of 10 improvement in machine accuracy. The machine was of the moving bridge configuration, as shown in Fig. 1. The bridge moves in the Y direction along an air bearing guideway on the table. A carriage, moveable in the X direction, is mounted on the bridge. The ram is mounted on the X carriage and moves in the Z direction. Probes are mounted on the end of the ram.

THE MACHINE MODEL

Our model of the machine is designed to compensate for the systematic geometric errors in the machine, and for first-order thermal expansions of the machine scales. The geometric errors are premeasured and stored for on-line correction, while the temperature of the machine scales is measured during operation.

Because we desired to keep the machine model as simple as possible, we used the rigid-body assumption to compute the machine geometry. This assumption is, of course, only an approximation which has caused us and other workers some difficulty in the past (Ref. 1 and 2). We therefore checked the largest contributor to non-rigid-body behavior (position-dependent bending of the machine table) before acquiring any other geometric data. In order to do this, the flatness of the table was measured for nine different positions of the bridge and X carriage (movement of the ram is not included since it is counterweighted). The chosen positions are shown in Fig. 2, and the worst case difference in flatness between two positions of ram and bridge is shown in Fig. 3. Except for positions very close to two corners of the table, the change in table flatness due to changing load distribution is less than 1 micrometer, which led us to believe that for this measuring machine a rigid-body model would be acceptable.

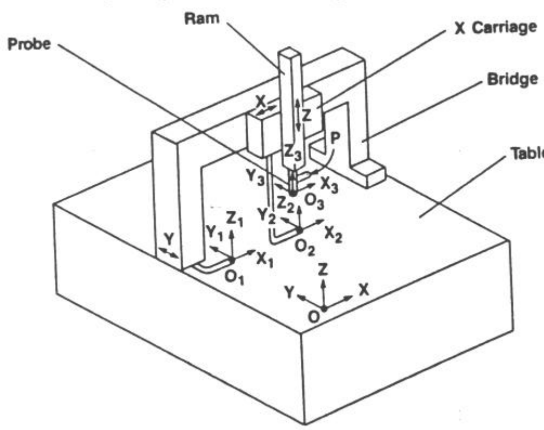

FIGURE 1. DIAGRAM OF THE COORDINATE MEASURING MACHINE

The model we used required four independent coordinate systems, as shown in Fig. 1. They are the table system (O,X,Y,Z), the bridge system (O_1,X_1,Y_1,Z_1), the X carriage system (O_2,X_2,Y_2,Z_2), and the ram system (O_3,X_3,Y_3,Z_3). For conceptual purposes, the bridge system and the X carriage system are shown in Fig. 1 as being attached to the bridge and X carriage, respectively, through small, non-existent connecting rods. We assume that at the beginning of motion all four origins coincide and the axes of all four systems are aligned. We also choose the Y axis as the starting line for squareness compensation (i.e., X is assumed out-of-square with Y) and the X-Y plane as the reference for Z squareness. The notation is similar to that introduced by Tlusty (Ref. 3) and expanded upon in Ref. 4. In this notation the subscript denotes the error direction and the argument the motion direction.

Thus, when the bridge moves a nominal distance Y, the actual position of the bridge origin O_1, in the table system, is given by the vector

$$\overrightarrow{OO_1} = \begin{pmatrix} \delta_x(Y) \\ Y - \delta_y(Y) \\ \delta_z(Y) \end{pmatrix} \qquad (1)$$

where the δ are used here to denote type F straightness (Ref. 4). At the same time, the whole bridge coordinate system rotates with respect to the table system due to the angular error motions. This rotation can be expressed by the infinitesimal rotation matrix

$$R_1 = \begin{pmatrix} 1 & \varepsilon_z(Y) & -\varepsilon_y(Y) \\ -\varepsilon_z(Y) & 1 & \varepsilon_x(Y) \\ \varepsilon_y(Y) & -\varepsilon_x(Y) & 1 \end{pmatrix} \qquad (2)$$

Similarly, when the X carriage moves a nominal distance X, and the ram moves a nominal distance Z, we have the two additional vectors

$$\overrightarrow{O_1O_2} = \begin{pmatrix} X - \delta_x(X) \\ -X\cdot\alpha + \delta_y(X) \\ \delta_z(X) \end{pmatrix} \qquad (3a)$$

$$\overrightarrow{O_2O_3} = \begin{pmatrix} -Z\cdot\beta_1 + \delta_x(Z) \\ -Z\cdot\beta_2 + \delta_y(Z) \\ Z - \delta_z(Z) \end{pmatrix} \qquad (3b)$$

where we have explicitly included the X-Y out-of-squareness as the angle α and the Z out-of-squareness to the X-Y plane as the two angles β_1 and β_2. The infinitesimal rotation matrices for these motions (R_2,R_3) can be readily generated from Eq. 2 by simply replacing the argument Y with X or Z, respectively.

Given the above definitions, the coordinates in the table system (X',Y',Z') of an arbitrary point P, which has coordinates (X_p,Y_p,Z_p) in the ram system, can be determined from the following equation:

$$\overrightarrow{OP} = \overrightarrow{OO_1} + R_1^{-1}(R_2^{-1}(R_3^{-1}\overrightarrow{O_3P} + \overrightarrow{O_2O_3}) + \overrightarrow{O_1O_2}) \qquad (4)$$

where the superscript -1 indicates the inverse matrix. Writing out Eq. 4 by coordinates yields the equations necessary for the geometric portion of the error compensation which are

$$\Delta X = -\delta_x(X) + \delta_x(Y) + \delta_x(Z) - Z\cdot\beta_1 + Z\cdot\varepsilon_y(X) + Z\cdot\varepsilon_y(Y)$$
$$- Y_p(\varepsilon_z(X) + \varepsilon_z(Y) + \varepsilon_z(Z)) + Z_p(\varepsilon_y(X) + \varepsilon_y(Y) + \varepsilon_y(Z)) \quad (5a)$$

$$\Delta Y = -\delta_y(Y) + \delta_y(X) + \delta_y(Z) - X\cdot\alpha - Z\cdot\beta_2 + X\cdot\varepsilon_z(Y) - Z\cdot\varepsilon_x(Y)$$
$$+ X_p(\varepsilon_z(X) + \varepsilon_z(Y) + \varepsilon_z(Z)) - Z_p(\varepsilon_x(X) + \varepsilon_x(Y) + \varepsilon_x(Z)) \quad (5b)$$
$$- Z\cdot\varepsilon_x(X)$$

$$\Delta Z = -\delta_z(Z) + \delta_z(X) + \delta_z(Y) - X\cdot\varepsilon_y(Y) - X_p(\varepsilon_y(X) + \varepsilon_y(Y) + \varepsilon_y(Z))$$
$$+ Y_p(\varepsilon_x(X) + \varepsilon_x(Y) + \varepsilon_x(Z)) \quad (5c)$$

where X, Y and Z as arguments refer to the nominal machine reading, $\Delta X = X - X' - X_p$, and similarly for the other coordinates.

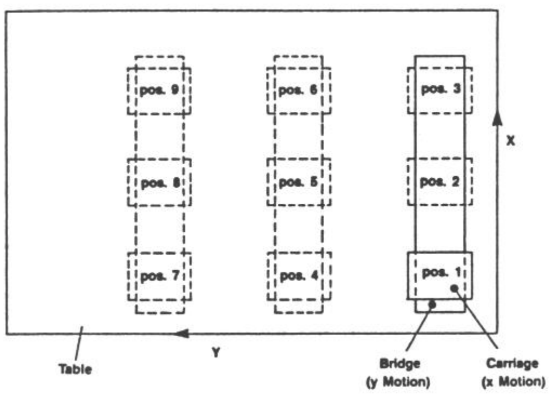

FIGURE 2. POSITIONS CHOSEN FOR POSITION-DEPENDENT TABLE BENDING MEASUREMENTS

In order to complete the model, we then added a correction for temperature. Since our machine was in a metrology laboratory temperature controlled to ±1 Celsius, simple compensation for scale changes was felt to be sufficient. Two thermistors were symmetrically mounted on each of the machine scales (which were glass line scales). The thermal error for each scale was assumed to be of the form

$$\Delta X_T = \alpha_x \cdot X\left(((T_1 + T_2)/2) - 20\right) \quad (6)$$

and similarly for Y and Z. Here α_x is the effective thermal expansion coefficient with that coordinate, T_1 and T_2 are the temperatures of the two thermistors, and 20, of course, is the standard metrological temperature in Celsius. (It should be noted that other more complicated models were tried, but the improvement in results was not sufficient to justify greater complexity.)

FIGURE 3. MAXIMUM DIFFERENCES IN TABLE FLATNESS (MICROMETERS)

The effective coefficient of expansion was found to be needed, however, as there were significant differences between the three scales as well as differences from the nominal expansion values for the scales. For this machine we obtained effective coefficients of 16, 10 and 13 parts per million per Celsius for the X, Y and Z scales, respectively. This was thought to be caused by the combination of the aluminum cases used to constrain the scales and internal stresses in the scales caused by screws which were used by the manufacturer to compress the scales and adjust their effective length.

The effective coefficient of expansion was obtained by measuring the scale error for each scale, at different temperatures, and obtaining the slope of the resulting lines. A typical curve for the X scale is shown in Fig. 4.

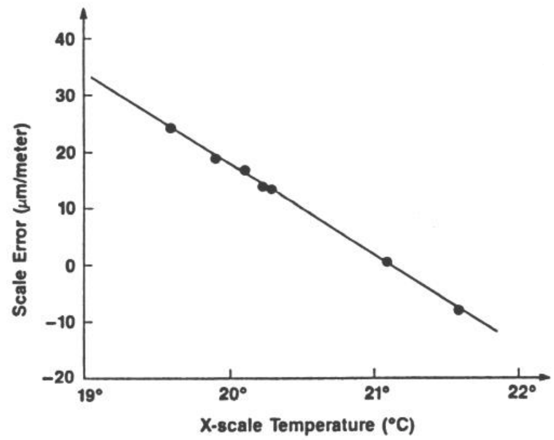

FIGURE 4. THERMAL BEHAVIOR OF THE MACHINE X SCALE

MACHINE GEOMETRIC CALIBRATION

In order to prepare the error tables for the correction of the geometric error of this measuring machine, all 21 error terms given in the previous section had to be measured. Scale errors, straightness errors, and the three angular errors per axis had to be measured along the whole travel of the given axis at regular intervals. Since these errors usually change gradually, we measured them every 50 millimeters for the X and Y axes, and every 20 millimeters for the Z axis. (The total measurement volume of the machine was 700 x 900 x 460 millimeters.) For all of these motions, all error terms except for angular rotation about the motion axis (often called "roll") were measured using a Hewlett-Packard laser interferometer compensated for environmental conditions (Ref. 5). Because of physical limitations on the optics, the plane Z=80 millimeters was chosen for making the X and Y measurements. Because of similar limitations for Z less than 80, the Z scale error had to be measured using gage blocks, and the pitch and yaw $(\varepsilon_x(Z), \varepsilon_y(Z))$ of this axis over this range measured using differential levels. The roll measurements for the X and Y axes $(\varepsilon_x(X), \varepsilon_y(Y))$ were performed using the same differential levels, while the Z roll was measured using a surface plate on its side and two offset electronic indicators, as shown in Fig. 5.

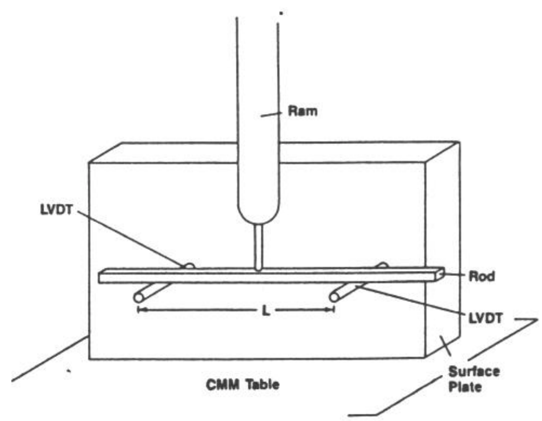

FIGURE 5. SETUP FOR MEASURING ROLL $(\varepsilon_z(Z))$ OF THE RAM AXIS

The above measurements yielded data on 18 of the required error terms; however, it was still necessary to measure the axis squareness of the machine, which is extremely important in determining the final accuracy. A common method, which uses an optical square (Ref. 6), was not used due to errors inherent in this approach (Ref. 7). Instead, we determined the squareness using a method common in surveying, that of measuring along machine diagonals. This proved to be an extremely sensitive and accurate method for squareness determination. For example, examine the setup for measuring X-Y squareness, which is shown in Fig. 6. Here the corner cube of the interferometer moves along the X-Y diagonal from X=0, Y=0 to X=700 mm, Y=900 mm. The distance traveled is given by

$$d_i = X_{ai} \sin\theta + y_{ai} \cos\theta \qquad (7)$$

where X_{ai} and Y_{ai} are the actual coordinates in the table frame of the end of the ram at the ith measured point. The error in displacement along the diagonal caused by X-Y squareness is

$$\Delta d_i = d_i - X_{ci} \sin\theta - Y_{ci} \cos\theta \qquad (8)$$

where X_{ci} and Y_{ci} are the coordinates of the ith measured point after compensation for scale, straightness and angular errors, but before taking into account the out-of-squareness of the X-Y axes. The compensated coordinates are related to the actual coordinates by

$$X_{ci} = X_{ai} + \Delta X_r \qquad (9a)$$

$$Y_{ci} = Y_{ai} + \Delta Y_r \qquad (9b)$$

where ΔX_r and ΔY_r are the residual errors after compensation for all but squareness. Thus the diagonal error (Eq. 8) is given by

$$\Delta d_i = -\Delta X_r \sin\theta - \Delta Y_r \cos\theta - Y_{ci}\,\alpha \sin\theta \qquad (10)$$

Fig. 7 is a graph of the diagonal error as a function of Y, as measured on this machine. The slope of the least-squares fit line to this curve is the out-of-squareness times the sine of theta. If the residual errors in X and Y and the uncertainty in the measurement of the error in the diagonal are totally random, then the uncertainty in the out-of-squareness measured by this technique would be less than 0.1 arc-second for this measurement. If, however, there were systematics left after the partial error compensation, then this error can be considerably larger. We therefore attempted to eliminate this systematic error by measuring a second diagonal nearly simultaneously, as shown in the figure. The slope of the resulting curve is opposite to that of the preceeding diagonal, and the average from these data sets gives the squareness error. This procedure, which is somewhat analogous to straightedge reversal, leads to the cancellation of many forms of systematic error. Details of the diagonal method for these types of measurements will be discussed elsewhere (Ref. 8).

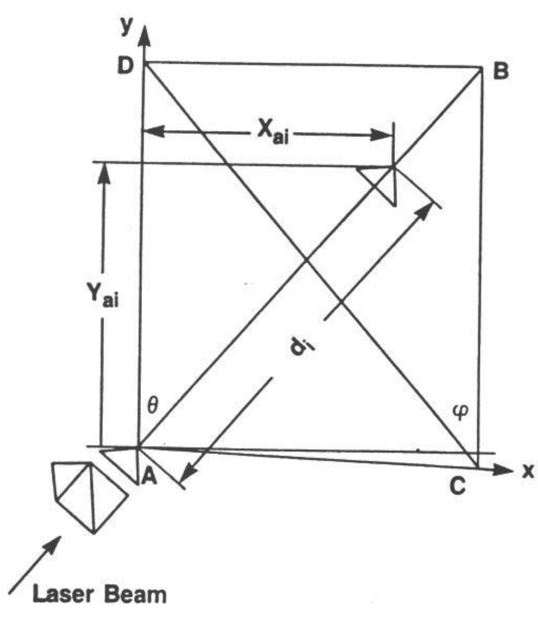

FIGURE 6. SETUP FOR DIAGONAL MEASUREMENTS

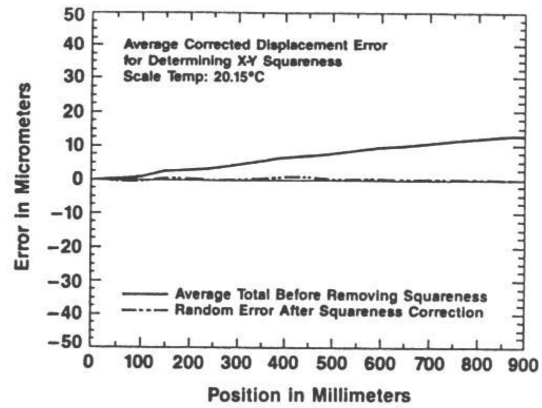

FIGURE 7. X-Y DIAGONAL ERROR AS A FUNCTION OF Y

SOFTWARE FOR ERROR COMPENSATION

The software to perform the compensation was added as a single subroutine in the control computer for the measuring machine, which was a small minicomputer. About 3 kbytes of memory were required for this subroutine. The subroutine required the operator to input the X, Y and Z offsets of the probe used, to input the reference coordinates for the zero point of the measurement system (this would not be required on a machine which had absolute encoders), and the scale and workpiece temperatures. During operation the subroutine then read the nominal machine coordinates, performed a linear interpolation to calculate the expected value for the 18 position-dependent error terms, and calculated the compensated coordinates using Eqs. 5 and 6. This routine also can readily be used to create error maps of the machine as built. Fig. 8 shows such an error map for the plane Z=30 at 20 Celsius. The maximum error in this plane occurs for measurements from point (100,900,30) to point (700,0,30) and has a value of 29.4 micrometers. When the temperature is decreased to 19 Celsius, the error between these two points increases approximately 10 micrometers. The largest error measured was 43 micrometers, at the lowest temperature that the lab reached.

CMM Error Map For Z=30 With Reference To (0,0,30) X,Y,Z Component Error in Micrometers : X Y Z

(Y mm) \ x mm	0	100	200	300	400	500	600	700
900	2 5 -1	1 10 -1	6 -4 1	9 -8 2	7 -7 3	7 -3 3	6 -9 5	14 -13 8
800	-0 5 1	-0 9 1	4 -4 3	7 -7 4	6 -7 4	6 -3 4	4 -8 7	12 -12 8
700	0 4 2	0 9 2	4 -5 4	7 -0 5	6 -7 5	6 -3 5	5 -8 7	13 -12 8
600	-0 2 3	-1 6 2	4 -7 4	7 -10 5	5 -10 4	5 -6 4	4 -11 6	12 -15 7
500	-0 -1 4	-0 3 3	4 -10 4	7 -13 5	6 -12 4	6 -8 3	4 -13 5	12 -17 6
400	0 -0 4	0 5 2	5 -9 4	7 -12 4	6 -11 4	6 -7 3	5 -12 4	13 -16 5
300	1 1 3	1 6 2	5 -8 3	8 -10 3	6 -10 3	7 -6 2	5 -11 3	13 -15 4
200	0 3 2	0 7 0	4 -7 1	7 -10 1	6 -10 1	6 -6 -0	5 -11 1	13 -16 2
100	-1 5 0	-1 9 -1	3 -5 0	5 -9 0	5 -9 -0	5 -5 -1	4 -11 -0	12 -15 1
0	0 0 0	-0 4 -1	4 -10 -0	7 -13 -0	6 -12 -1	6 -9 -2	4 -14 -1	12 -10 0

FIGURE 8. CMM ERROR MAP

RESULTS

The efficacy of the error compensation was tested in two ways: first by performing linear positioning tests on more than 50 lines along different directions within the work zone; and second by measuring a calibrated gage block.

The results of some of the linear measurements are given in Figs. 9, 10 and 11. Fig. 9 shows the results on an X-Y diagonal of the machine. The total uncompensated error was 31.1 micrometer, and after compensation the error was 2.5 micrometers. For analysis purposes, we divided the error into linear components, that is, the portion of the error that can be accounted for by a best-fit straight line, and non-linear components, which are the residuals obtained after subtracting the best-fit straight line from the error. An examination of the data in Fig. 9 shows that the maximum non-linear portion was only -0.76 micrometer, while the linear portion of the residual after correction was considerably larger. This linear component could be caused by error in the temperature measurement, in the determination of the effective coefficient of expansion, in the squareness measurement, or perhaps a change in squareness in the time between calibration and testing.

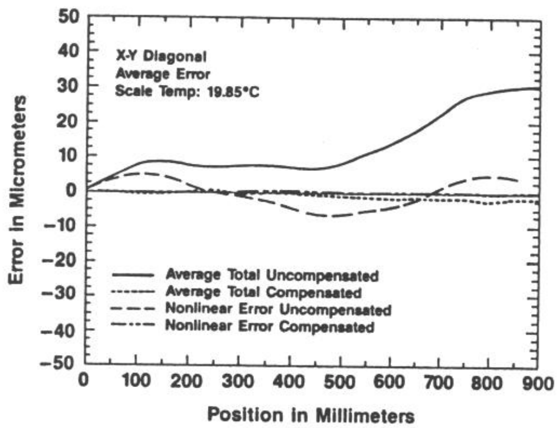

FIGURE 9. ERROR MEASUREMENTS ON AN X-Y DIAGONAL

In Fig. 10 another result is shown for an X-Y-Z diagonal. The total error before compensation is 42 micrometers and after it is -1.3 micrometers. Our worst-case result is shown in Fig. 11 for another X-Y-Z diagonal. Here the maximum error is 4.7 micrometers before compensation and -4 micrometers after compensation. In summary, however, we found that among all measured lines more than 20 percent had total error greater than 20 micrometers before compensation, but after compensation less than 20 percent of the lines had a maximum error larger than 2 micrometers. Thus, on the whole, we obtained an improvement in machine accuracy by more than a factor of ten, with the maximum error over the full work zone being reduced from more than 40 micrometers to less than 4 micrometers.

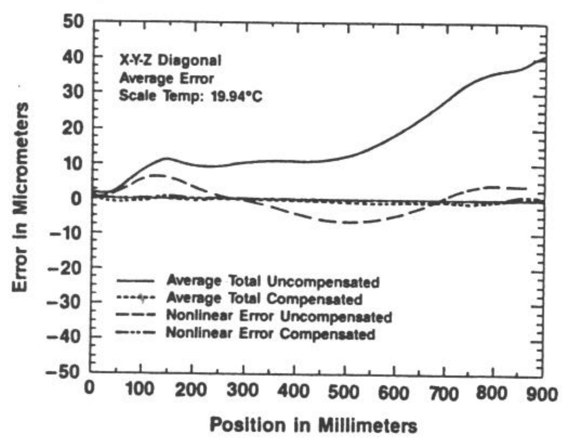

FIGURE 10. ERROR MEASURED ON AN X-Y-Z DIAGONAL

The error compensation was also tested by measuring a 20.3-inch (515 millimeters) gage block in a variety of positions. The block was mounted on a sine bar so that it could be oriented at different angles, and the machine touch-fire probe was replaced by an LVDT. Two thermocouples were mounted on the gage block to measure the workpiece temperature. The results of these measurements are shown in the following table. The maximum error obtained before compensation was 7.5 micrometers and after compensation was 1.4 micrometers. All measurements were performed at 20 ± 0.5 Celsius, which, because of the large thermal corrections required on this machine, reduces the error before compensation.

Summary of 20.3-in. Gage Block Measurements

Position	Uncompensated Error (micrometers)	Compensated Error (micrometers)
1	-4.7	-1.2
2	-2.9	0.5
3	-3.0	0.3
4	-5.4	-0.1
5	-7.5	1.4
6	0.4	-0.7
7	2.6	1.2

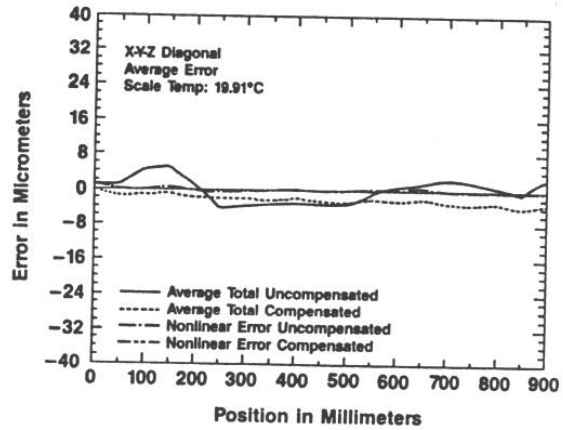

FIGURE 11. ERROR MEASURED ON AN X-Y-Z DIAGONAL

CONCLUSIONS

The results above lead us to conclude that error compensation is a powerful and economical way to upgrade the accuracy of coordinate measuring machines. It is clearly possible to obtain a factor of 10 or more improvement if compensation is done conscientiously. Obtaining such improvement requires a correct geometric model, a correct thermal model, and careful machine calibration. We found particular attention had to be paid to squareness and angle errors, as well as to the machine scales and thermal behavior. It also seems possible that error compensation techniques could yield even more benefits if they were considered at the design stage of a measuring machine, as has been done for special purpose machine tools (Ref. 9). If this were done, then the main design criteria for a machine would be repeatability and stability, and other requirements, such as precise alignment and adjustment mechanisms, could be relaxed.

REFERENCES

1. R. Hocken, et al., "Three Dimensional Metrology", Annals of the CIRP 26/2 (1977).

2. R. Schultschik, "The Accuracy of Machine Tools Under Load Conditions", Annals of the CIRP 28/1 (1979).

3. J. Tlusty, "Testing of Accuracy of Machine Tools" (Supplement to the Machine Tool Task Force Report), UCRL-529-Supplement 1 (1980).

4. R. Hocken, "Technology of Machine Tools, Vol. 5: Machine Tool Accuracy", Report of the Machine Tool Task Force, UCRL-52960-5 (1980).

5. NBS Communications Manual for Scientific, Technical and Public Information (November 1980), p. 9 & 10, "Certain commercial equipment, instruments, or materials are identified in this paper in order to adequately specify the experimental procedure. Such identification does not imply recommendation or endorsement by the National Bureau of Standards, nor does it imply that the materials or equipment identified are necessarily the best available for the purpose."

6. Hewlett-Packard Publication, Laser Measurement System Application Note 154-6, "Calibration of a Machine Tool".

7. G. Zhang and R. Veale, "Error of the Effective Angle of Refraction by a Pentaprism Due to Misalignment", in preparation.

8. G. Zhang and R. Veale, "Displacement Method for Machine Geometry Calibration", in preparation.

9. For example, see R. R. Donaldson, "Error Budgets", Report of the Machine Tool Task Force, Vol. 5: "Machine Tool Accuracy", UCRL-52960-5 (1980).